

## MRI Sensing Based on the Displacement of Paramagnetic Ions from Chelated Complexes

Tatjana Atanasijevic, Xiao-an Zhang,\* Stephen J. Lippard,\* and Alan Jasanoff\*

*Departments of Biological Engineering and Chemistry, Massachusetts Institute of Technology, 150 Albany Street, NW14-2213, Cambridge, Massachusetts 02139*

Received January 25, 2010

We introduce a mechanism for ion sensing by MRI in which analytes compete with paramagnetic ions for binding to polydentate chelating agents. Displacement of the paramagnetic ions results in alteration of solvent interaction parameters and consequent changes in relaxivity and MRI contrast. The MRI changes can be tuned by the choice of chelator. As an example, we show that calcium-dependent displacement of  $\text{Mn}^{2+}$  ions bound to EGTA and BAPTA results in a  $T_1$ -weighted MRI signal increase, whereas displacement from calmodulin results in a signal decrease. The changes are ion selective and can be explained using relaxivity theory. The ratio of  $T_2$  to  $T_1$  relaxivity is also calcium-dependent, indicating the feasibility of “ratiometric” analyte detection, independent of the probe concentration. Measurement of paramagnetic ion displacement effects could be used to determine analyte ion concentrations with spatial resolution in opaque specimens.

A variety of mechanisms have been proposed for detecting inorganic ions using magnetic resonance imaging (MRI) contrast agents. In the most widely explored approach, analyte binding to a paramagnetic metal chelate withdraws ligands, increasing the number ( $q$ ) of inner-sphere sites available for water coordination at the paramagnetic center. As a consequence, the longitudinal relaxivity ( $r_1$ ) of protons on exchangeable solvent molecules in the complex is similarly increased.<sup>1</sup> Here we introduce a new strategy in which the analyte completely releases the paramagnetic ion from a polydentate chelating ligand to form the aqua complex (aq), which serves as an efficient MRI contrast agent with characteristics sharply different from those of the chelate. In this facile and flexible new approach, changes in  $r_1$  can be tuned by the choice of the metal chelate complex (Figure 1a). Measurement of the effect by MRI can then be used to determine the analyte concentration with spatiotemporal resolution.

We tested the applicability of the paramagnetic metal displacement strategy to sense calcium ions by MRI. We

chose the relatively labile manganese(II) ion as the paramagnetic reporter because aqueous  $\text{Mn}^{2+}$  is widely used as a  $T_1$  contrast agent for in vivo imaging.<sup>2</sup> Manganese complexes were assembled with ethylene glycol bis( $\beta$ -aminoethyl ether)- $N,N,N',N'$ -tetraacetic acid (EGTA), 1,2-bis(*o*-aminophenoxy)ethane- $N,N,N',N'$ -tetraacetic acid (BAPTA), and calmodulin (CaM), all metal-binding molecules with selective affinity for  $\text{Ca}^{2+}$  ions. Structures of  $\text{Mn}^{2+}$  associated with EGTA<sup>3</sup> and with a protein domain closely related to the four calcium-binding regions of CaM<sup>4</sup> are shown in Figure 1b,c. They suggest that from zero to two coordinated water molecules per  $\text{Mn}^{2+}$  ion may be present. In contrast,  $\text{Mn}^{2+}(\text{aq})$  is coordinated by six water molecules.<sup>5</sup> These differences in  $q$ , combined with rotational correlation time ( $\tau_R$ ) effects and the time constant for water exchange ( $\tau_M$ , where  $q \neq 0$ ), contribute to relaxivity changes upon displacement of  $\text{Mn}^{2+}$  bound by EGTA, BAPTA, or CaM, upon addition of  $\text{Ca}^{2+}$ .

Mixtures containing 100  $\mu\text{M}$   $\text{Mn}^{2+}$  in 1:1 stoichiometry with EGTA or BAPTA, or in 4:1 stoichiometry with CaM, which has four metal binding sites, were imaged in the presence of 0–20 mM  $\text{CaCl}_2$ , using spin-echo pulse sequences in a 4.7 T MRI scanner at room temperature (22 °C). In all cases, progressive changes in the MRI signal were observed as  $\text{Ca}^{2+}$  concentrations increased (Figure 2a). Controls lacking  $\text{Mn}^{2+}$  or chelators showed no significant changes (Supporting Information). Intensity data were analyzed to determine relaxivity as a function of the  $\text{Ca}^{2+}$  concentration for each chelator (Figure 2b). As  $[\text{Ca}^{2+}]$  increased, values of  $r_1$  increased from 1.7 to 5.2  $\text{mM}^{-1} \text{s}^{-1}$  for EGTA and from 1.3 to 6.2  $\text{mM}^{-1} \text{s}^{-1}$  for BAPTA (estimated errors 10%). For CaM,  $r_1$  decreased from 10.5 to 5.5  $\text{mM}^{-1} \text{s}^{-1}$  with increasing  $[\text{Ca}^{2+}]$ . Changes in the transverse relaxation rate ( $r_2$ ) were also observed (Figure 2c). Addition of  $\text{Ca}^{2+}$  to Mn-EGTA or Mn-BAPTA produced  $r_2$  increases from 19 or 8.6  $\text{mM}^{-1} \text{s}^{-1}$ , respectively, to 92 or 98  $\text{mM}^{-1} \text{s}^{-1}$ . Addition of  $\text{Ca}^{2+}$  to  $\text{Mn}_4\text{CaM}$  induced a modest drop in the apparent transverse relaxivity, from

(2) Koretsky, A. P.; Silva, A. C. *NMR Biomed.* **2004**, *17*, 527–531.

(3) Schauer, C. K.; Anderson, O. P. *Acta Crystallogr., Sect. C* **1988**, *44*, 981–986.

(4) Andersson, M.; Malmendal, A.; Linse, S.; Ivarsson, I.; Forsen, S.; Svensson, L. A. *Protein Sci.* **1997**, *6*, 1139–1147.

(5) Lauffer, R. B. *Chem. Rev.* **1987**, *87*, 901–927.

\*To whom correspondence should be addressed. E-mail: xazhang@utsc.utoronto.ca (X.Z.), lippard@mit.edu (S.J.L.), jasanoff@mit.edu (A.J.).

(1) Li, W.; Fraser, S. E.; Meade, T. J. *J. Am. Chem. Soc.* **1999**, *121*, 1413–1414.

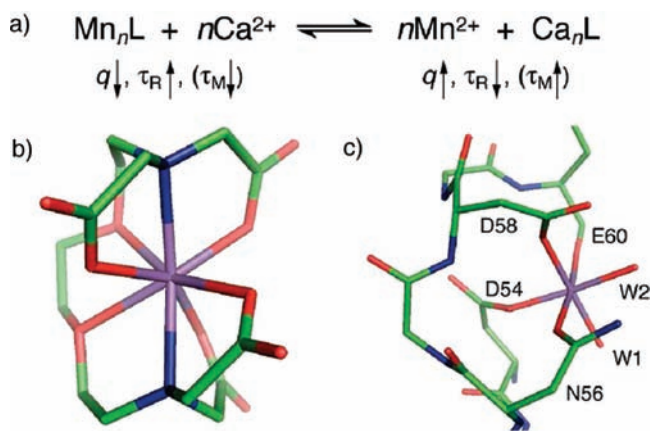


**Figure 1.** Mechanism of MRI calcium sensors based on displacement of  $\text{Mn}^{2+}$  from chelated complexes. (a) Upon addition of excess  $\text{Ca}^{2+}$ ,  $\text{Mn}^{2+}$  ions are released from ligand molecules (L) including EGTA, BAPTA, and CaM. Dissociated  $\text{Mn}^{2+}$  ions have higher  $q$ , lower  $\tau_R$ , and, for L = CaM, higher  $\tau_M$  than chelated manganese, all factors that influence longitudinal relaxivity. (b) In the complex with EGTA,  $\text{Mn}^{2+}$  (purple) is octacoordinate with  $q = 0$ .<sup>2</sup> (c) The crystal structure of  $\text{Mn}^{2+}$  in the complex with a canonical calcium binding site, loop 2 of calbindin,<sup>4</sup> shows two bound waters (W1 and W2); this binding loop has 71% sequence identity to the corresponding seven residues in the first EF hand of CaM, suggesting that  $\text{Mn}^{2+}$  ions in the complex with CaM may similarly exhibit  $q = 2$ .

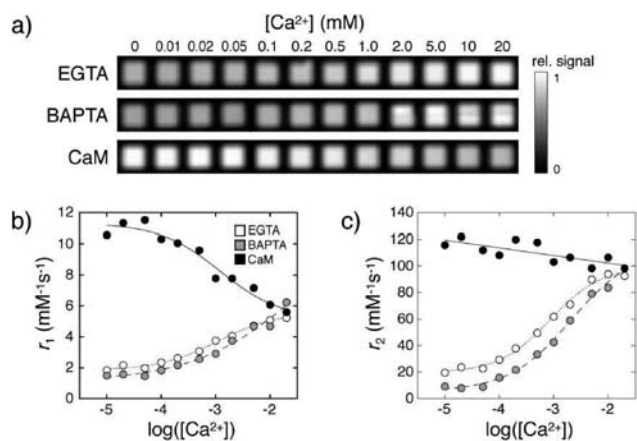


**Figure 2.** MRI and relaxivity changes upon paramagnetic displacement from chelators. (a) Progressive  $T_1$ -weighted MRI signal changes observed as a function of  $[\text{Ca}^{2+}]$  added to mixtures of  $100 \mu\text{M}$   $\text{Mn}^{2+}$  with  $100 \mu\text{M}$  EGTA,  $100 \mu\text{M}$  BAPTA, or  $25 \mu\text{M}$  CaM, all in MOPS, pH 7. Intensity changes were normalized to the maximal MRI signal across the titration range. (b) Longitudinal relaxivities ( $r_1$ ) computed from  $T_1$ -weighted data, as a function of calcium concentrations for Mn-EGTA (open circles), Mn-BAPTA (gray circles), and  $\text{Mn}_4\text{CaM}$  (black circles). Fitted curves are shown for visualization purposes. (c) Transverse relaxivity ( $r_2$ ) for the same samples.

$110$  to  $98 \text{ mM}^{-1} \text{ s}^{-1}$ . All three ligands showed substantial calcium-dependent changes in  $r_2/r_1$  (Supporting Information), suggesting that these reagents and their derivatives might be used to probe concentration-independent “ratio-metric” quantification of  $[\text{Ca}^{2+}]$  or other divalent cations.<sup>6,7</sup>

The titration curves produced by adding  $\text{Ca}^{2+}$  to  $\text{Mn}^{2+}$  mixtures with EGTA, BAPTA, or CaM converged on

relaxivity values similar to those measured using  $\text{Mn}^{2+}(\text{aq})$  complexes ( $r_1 = 5.6 \pm 0.1 \text{ mM}^{-1} \text{ s}^{-1}$  and  $r_2 = 98 \pm 3 \text{ mM}^{-1} \text{ s}^{-1}$ ), supporting the conclusion that the relaxation changes were caused by the  $\text{Ca}^{2+}$ -dependent  $\text{Mn}^{2+}$  displacement mechanism. A  $20 \text{ mM}$   $\text{Ca}^{2+}$  concentration brought about almost complete  $\text{Mn}^{2+}$  dissociation in all cases. This result is in reasonable agreement with reported values of  $K_d(\text{Mn}^{2+})/K_d(\text{Ca}^{2+})$  for EGTA of  $10^{-1.3}$  and for BAPTA of  $10^{-2.8,9}$ . The  $\text{Ca}^{2+}$ -induced  $r_1$  increases observed for Mn-EGTA and Mn-BAPTA were also consistent with the anticipated effects of increasing  $q$  of  $\text{Mn}^{2+}$  from zero to six following displacement of the ion from the chelators. Relaxivities of Mn-EGTA and Mn-BAPTA complexes measured in the absence of calcium were comparable to outer-sphere relaxivities reported at different fields for other  $\text{Mn}^{2+}$  complexes having  $q = 0$ .<sup>10–12</sup> Ironically, the low relaxivities and relatively labile nature of many  $q = 0$   $\text{Mn}^{2+}$  complexes have historically been considered a limitation to their use as contrast agents in clinical MRI, but these very properties have been exploited here to enable calcium sensing based on displacement of  $\text{Mn}^{2+}$  from Mn-EGTA and Mn-BAPTA.

The structure and nuclear magnetic relaxation properties of  $\text{Mn}_4\text{CaM}$  have not been previously studied, but inner-sphere contributions to  $r_1$  of the CaM complex can be estimated, in conjunction with experimentally justified values for  $\tau_M$  and  $\tau_R$  (see the Supporting Information). The modeling studies indicate that the  $T_1$  relaxivity per bound water ( $r_1/q$ ) for  $\text{Mn}_4\text{CaM}$  is approximately 10-fold higher than for  $\text{Mn}^{2+}(\text{aq})$ . Both a short  $\tau_M$ , as generally reported for  $q \neq 0$   $\text{Mn}^{2+}$  complexes,<sup>5</sup> and long  $\tau_R$  for  $\text{Mn}_4\text{CaM}$  probably account for its strong relaxation effects and counterbalance its reduced  $q$ , compared to  $\text{Mn}^{2+}(\text{aq})$ . The shape of the CaM titration curve thus reflects multiple determinants of  $r_1$ , in addition to contributions of  $\text{Mn}^{2+}/\text{Ca}^{2+}$  exchange at all of the four protein metal-binding sites. The CaM titration data were well approximated ( $r = 0.98$ ) by a monophasic binding curve with a Hill coefficient of 0.8, suggesting that metal substitution at each site was approximately independent and identically distributed.

To explore the analyte selectivity, we measured relaxivity changes of  $\text{Mn}^{2+}$  complexes in the presence of diamagnetic competitor ions of biological relevance. Excesses of  $\text{Zn}^{2+}$ ,  $\text{Mg}^{2+}$ , or  $\text{K}^+$  (each  $1 \text{ mM}$ ) were added to  $100 \mu\text{M}$   $\text{Mn}^{2+}$  in stoichiometric mixtures with metal-binding sites in EGTA, BAPTA, or CaM. As predicted by reported affinity constants<sup>8,9</sup> and the Irving–Williams series,  $\text{Zn}^{2+}$  produced strong  $r_1$  changes in Mn-EGTA and Mn-BAPTA and abolished calcium sensitivity, but  $\text{Mg}^{2+}$  and  $\text{K}^+$  had little effect (Figure 3a–c). Calcium-induced longitudinal relaxation ( $T_1$ ) changes on  $\text{Mn}_4\text{CaM}$  persisted in the presence of the competitor ions, but both  $\text{Zn}^{2+}$  and  $\text{Mg}^{2+}$  reduced calcium-dependent effects. Competitive effects on calcium-dependent transverse relaxation ( $T_2$ ) changes followed a similar pattern

(8) Cheng, K. L.; Ueno, K.; Imamura, T. *CRC Handbook of Organic Analytical Reagents*; CRC Press: Boca Raton, FL, 1982.

(9) Yuchi, A.; Tanaka, A.; Hirai, M.; Yasui, T.; Wada, H.; Nakagawa, G. *Bull. Chem. Soc. Jpn.* **1993**, *66*, 3377–3381.

(10) Elizondo, G.; Fretz, C. J.; Stark, D. D.; Rocklage, S. M.; Quay, S. C.; Worah, D.; Tsang, Y. M.; Chen, M. C.; Ferrucci, J. T. *Radiology* **1991**, *178*, 73–78.

(11) Troughton, J. S.; Greenfield, M. T.; Greenwood, J. M.; Dumas, S.; Wiethoff, A. J.; Wang, J.; Spiller, M.; McMurry, T. J.; Caravan, P. *Inorg. Chem.* **2004**, *43*, 6313–6323.

(12) Wang, S.; Westmoreland, T. D. *Inorg. Chem.* **2009**, *48*, 719–727.

(6) Gryniewicz, G.; Poenie, M.; Tsien, R. Y. *J. Biol. Chem.* **1985**, *260*, 3440–3450.

(7) Aime, S.; Fedeli, F.; Sanino, A.; Terreno, E. *J. Am. Chem. Soc.* **2006**, *128*, 11326–11327.

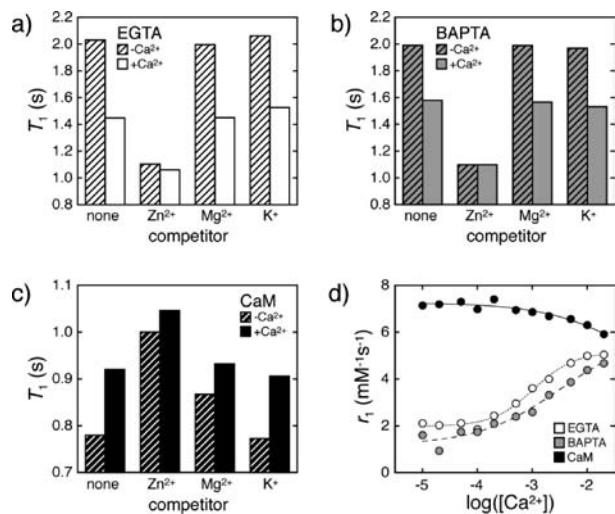


**Figure 3.** Calcium-dependent  $T_1$  changes recorded in the presence of competitor ions. Data obtained from  $100\ \mu M$   $Mn^{2+}$  mixtures with (a)  $100\ \mu M$  EGTA, (b)  $100\ \mu M$  BAPTA, or (c)  $25\ \mu M$  CaM, in the absence or presence of competing diamagnetic cations (each  $1\ mM$ ) and in the absence (striped bars) or presence (solid bars) of  $1\ mM$   $Ca^{2+}$ . (d) Titration of  $Ca^{2+}$  against Mn-EGTA, Mn-BAPTA, or  $Mn_4CaM$  in artificial cerebrospinal fluid (aCSF), showing the effects of biomimetic ion concentrations on titration curves.  $Mn^{2+}$ ,  $Ca^{2+}$ , and binding ligand concentrations as in Figure 2b. Note that  $1\ mM$   $Ca^{2+}$  did not bring about maximal relaxivity changes for any of the ligands.  $1\ mM$   $Zn^{2+}$  was more effective at displacing  $Mn^{2+}$  than  $1\ mM$   $Ca^{2+}$ , and therefore resulted in larger relaxation changes for all three chelators. The biologically relevant competitors  $Mg^{2+}$  and  $K^+$  did not alter calcium responses observed for Mn-EGTA and Mn-BAPTA, however, and  $Mg^{2+}$  only partially attenuated the  $Mn_4CaM$  response to  $1\ mM$   $Ca^{2+}$ .

for all three  $Mn^{2+}$  complexes (Supporting Information). As an additional test, we examined the calcium-induced relaxation changes induced in aCSF, a biomimetic solution approximating the interstitial environment of the brain (Figure 3d). The paramagnetic  $Mn^{2+}$  displacement effect for EGTA and BAPTA was minimally perturbed by the presence of competing solution components. For  $Mn_4CaM$ ,  $Ca^{2+}$ -dependent  $r_1$  changes were reduced and occurred at higher  $[Ca^{2+}]$ , perhaps reflecting the relatively high concentration ( $0.8\ mM$ ) of  $Mg^{2+}$  in aCSF.

These results indicate that the  $Mn^{2+}$  displacement mechanism for measuring  $Ca^{2+}$  or other ion concentrations by MRI provides strong contrast changes and could be useful for applications in solution, as well as in relatively simple naturalistic environments where few extraneous metal ligands are present.<sup>13</sup> A particular strength of the approach is the potential for ratiometric measurements. An obvious limitation in complex contexts is the possibility that paramagnetic metal ions, once released from the chelators, might diffuse away or be sequestered by binding partners unassociated with a sensing mechanism. This problem could be particularly serious where reversible or dynamic measurements are desired. A possible solution would be to use steady-state infusion or dialysis methods to maintain the concentration of paramagnetic complexes to a fixed level, ensuring that any analyte-induced metal dissociation and MRI contrast changes are reversed over time. In cases where the displaced paramagnetic ion is relatively nontoxic, these approaches might conceivably be applied in live animals. We note that the sensitivity range of the complexes studied here is ideally suited to detecting millimolar calcium concentrations present in extracellular compartments like the cerebral interstitium.<sup>14</sup> In the future, extensions of the paramagnetic metal displacement mechanism might include sensing of other ions, such as  $Zn^{2+}$  or  $Mg^{2+}$ , or the design of novel paramagnetic ion/chelator pairs, for example based on engineered CaM variants, with improved selectivity and sensitivity for detecting analytes by MRI.

**Acknowledgment.** This research was funded by NIH Grant DP2-OD2441 (New Innovator Award) to A.J., NIH Grant R01-GM65519 to S.J.L., and a grant from the McGovern Institute Neurotechnology Program to A.J. and S.J.L.

**Supporting Information Available:** Experimental details, additional results from control relaxation measurements, ratiometric data, relaxivity modeling, and selectivity data. This material is available free of charge via the Internet at <http://pubs.acs.org>.

(13) Manz, B.; Hillgartner, M.; Zimmermann, H.; Zimmermann, D.; Volke, F.; Zimmermann, U. *Eur. Biophys. J.* **2004**, *33*, 50–58.

(14) Angelovski, G.; Fouskova, P.; Mamedov, I.; Canals, S.; Toth, E.; Logothetis, N. K. *ChemBioChem* **2008**, *9*, 1729–1734.